machines

MDPI

Article

Hybrid One-Dimensional Convolutional Neural Network—Recurrent Neural Network Model for Reconstructing Missing Data in Structural Health Monitoring Systems

Nguyen Thi Thu Nga [1], Jose C. Matos [2] and Son Dang Ngoc [2,*]

[1] Resilience & Innovative Materials for smArt infraStructures (RIMAS), University of Transport Technology, 54 Trieu Khuc Street, Thanh Liet Ward, Hanoi 11407, Vietnam
[2] Department of Civil Engineering, ISISE, ARISE, University of Minho, 4800-058 Guimarães, Portugal
* Correspondence: sondn@civil.uminho.pt

Abstract

Data loss is a recurring and critical issue in Structural Health Monitoring (SHM) systems, often arising from a range of factors including sensor malfunction, communication breakdown, and exposure to adverse environmental conditions. Such interruptions in data availability can significantly compromise the accuracy and reliability of structural performance assessments, thereby hindering effective decision-making in safety evaluation and maintenance planning. In this study, a novel deep learning-based framework is proposed for data reconstruction in SHM, employing a hybrid architecture that integrates one-dimensional convolutional neural networks (1D-CNNs) with recurrent neural networks (RNNs). By combining these complementary strengths, the hybrid 1D-CNN–RNN model demonstrates superior capacity for accurate signal reconstruction. A real-world case study was conducted using vibration data from the Trai Hut Bridge in Vietnam. Five network configurations with varying depths were examined under single- and multi-channel loss scenarios. The results confirm that the method can accurately reconstruct lost signals. For single-channel loss, the best configuration achieved an MAE = 0.019 m/s^2 and R^2 = 0.987, while for multi-channel loss, a deeper network yielded an MAE = 0.044 m/s^2 and R^2 = 0.974. Furthermore, the model exhibits robust and stable performance even under more demanding multi-channel data loss conditions, highlighting its resilience to practical operational challenges. The results demonstrate that the proposed CNN–RNN framework is accurate, robust, and adaptable for practical SHM data reconstruction applications.

Keywords: SHM; deep learning; data loss; data reconstruction; hybrid 1D-CNN–RNN

check for updates

Academic Editor: Izaz Raouf

Received: 12 October 2025
Revised: 23 November 2025
Accepted: 26 November 2025
Published: 27 November 2025

Citation: Nga, N.T.T.; Matos, J.C.; Ngoc, S.D. Hybrid One-Dimensional Convolutional Neural Network—Recurrent Neural Network Model for Reconstructing Missing Data in Structural Health Monitoring Systems. *Machines* **2025**, *13*, 1101. https://doi.org/10.3390/machines13121101

Copyright: © 2025 by the authors. Licensee MDPI, Basel, Switzerland. This article is an open access article distributed under the terms and conditions of the Creative Commons Attribution (CC BY) license (https://creativecommons.org/licenses/by/4.0/).

1. Introduction

Large-scale projects are constantly being built and completed with complex structures and increasing social importance. To ensure the safe and efficient operation of these projects, SHM systems are often deployed from the early stages of the project [1,2]. The SHM system has become an essential tool for important projects such as bridges, hydroelectric dams and large buildings [3]. The SHM system allows early detection of damage and provides warnings about the condition of the project [4,5]. Based on the analysis results from the SHM system, management units can easily make decisions on repairing or maintaining the project [6]. It not only helps ensure safety but also minimises the cost of project repair [7,8]. Thanks to the advantages of the SHM system, projects can extend their lifespan and improve their performance. By deploying dense sensor networks, SHM systems enable engineers to

detect damage at an early stage and evaluate structural performance under various loads, supporting maintenance and rehabilitation decisions [9]. Sohn et al. [10] provided a comprehensive review of vibration-based damage detection methods. Farrar and Worden [11] introduced machine learning methods to enhance automated condition assessment. More recent studies have extended SHM applications to large-span bridges, using dense sensor arrays for modal recognition, vibration analysis, and damage localization [12,13].

The effectiveness of any SHM system is strongly dependent on the quality and continuity of the signals collected by its sensors [14]. Reliable vibration and acceleration measurements are essential for accurate modal identification, damage detection, and performance assessment [15]. However, issues like sensor failure, power outages, connection errors, or unfavourable climatic conditions can lead to data loss or corruption. In addition to interfering with ongoing monitoring, missing data drastically lowers the precision and dependability of structural assessment findings. The presence of noise, calibration errors, environmental disturbances, and sensor malfunctions can degrade the fidelity of recorded signals, leading to inaccurate estimates [16]. Data are more likely to be interrupted due to power outages, cable breaks, etc. It significantly hinders the ability of SHM systems to provide consistent and reliable information. Therefore, ensuring the availability of high-quality sensor signals is a prerequisite for achieving the full potential of SHM [17]. Effective strategies for reconstructing incomplete data are critical to maintaining system robustness and reliability [1,18].

Recently, a wide range of data reconstruction methodologies has been proposed to address the problem of missing data in structural health monitoring. Research has developed many strategies to address the problem of missing/loss data. These strategies can be divided into three categories: (i) data discarding methods; (ii) Statistical and probabilistic methods; (iii) Artificial intelligence methods. In the first category, corrupted or incomplete samples are removed prior to analysis to ensure that only reliable data are used. Such methods are straightforward and effective when the proportion of missing data is small. However, when data loss becomes significant, discarding large portions of the dataset leads to severe information reduction, which can damage bias detection and degrade the reliability of SHM outcomes. In order to improve the monitoring of structural dynamic reactions, Chen et al. [19] suggested an outlier elimination technique in which the dataset was restored and used for monitoring, following the implementation of this technique. Additionally, Laencina et al. [20] examined a number of data removal techniques for instances of inaccurate or missing data, stressing both their benefits and drawbacks. In general, data reduction techniques lead to decreased reliability and information loss. They work very well, though, in situations when there is a lot of data and little computing power.

For the second category, these approaches estimate missing values by exploiting temporal continuity and stochastic properties of the signals. Examples include interpolation techniques, autoregressive (AR/ARIMA) models, Kalman filtering, Bayesian estimation, and, more recently, matrix completion and low-rank approximation [21]. Kalman filters and Bayesian models can incorporate measurement uncertainty and provide recursive estimates of missing values [22], while matrix completion leverages spatial correlations across multiple sensor channels to recover large portions of missing data [23]. Although these methods have a solid theoretical foundation and are efficient in many cases, they generally assume linearity or stationarity and thus struggle with nonlinear and complex dynamic responses, particularly when data losses are long, irregular, or involve multiple channels [20,24]. Probabilistic and Bayesian-based approaches have gained increasing attention for processing incomplete or uncertain SHM data. These methods formulate the reconstruction or prediction task as a probabilistic inference problem, where missing or noisy measurements are treated as random variables with prior distributions. Such

Bayesian frameworks demonstrate strong potential for SHM applications, particularly when dealing with sensor data uncertainty and missing measurements [25,26].

The final category focuses on artificial intelligence applications. Artificial intelligence (AI) systems are able to identify patterns, thereby performing data reconstruction and accurate predictions through learning from curated time-series data [27]. The quality and dependability of the rebuilt data are enhanced by the simultaneous capacity of ML algorithms to handle heterogeneous and noisy data. By automating data processing operations, such as noise filtering and analysis, ML enables data reconstruction jobs while increasing efficiency and reducing errors [28,29].

Convolutional Neural Networks (CNNs) have shown remarkable performance in learning spatially correlated patterns from structural response data. In SHM, 1D-CNN architectures are capable of extracting local temporal and frequency-domain features directly from acceleration or strain signals, while higher convolutional layers integrate these into global representations related to modal behaviour or damage indicators. This capacity to learn multi-level features without manual preprocessing has made CNNs highly suitable for vibration-based SHM. Moreover, CNNs can effectively utilise correlations among multiple sensors, which is particularly advantageous in cases of partial data loss or sensor malfunction. Previous studies have demonstrated their success in applications such as modal identification, anomaly detection, and damage localisation. For SHM data reconstruction tasks, advanced neural network methodologies, which constitute the core of modern machine learning, represent some of the most promising approaches [30,31]. To reconstruct strain measurements for structural health monitoring (SHM) while considering the influence of temperature effects, Chen et al. [32] proposed employing a deep learning–autoregressive (DL–AR) approach. Their findings showed that the suggested model performed well and was accurate. Convolutional neural networks (CNNs) were presented and used to forecast the long-term strain data of concrete buildings in a different study [33]. Additionally, Lei et al. [34] described a technique for reconstructing lost SHM data that makes use of deep convolutional generative adversarial networks. Nguyen et al. [35–37] used different deep learning techniques to recover accelerometer sensor data. The results show the potential of DL in the task of sensor data reconstruction. The capability and effectiveness of deep learning in structural health monitoring data reconstruction have likewise been demonstrated in numerous further studies [38–40]. Hybrid architectures that combine CNNs with RNNs or attention mechanisms have shown improved accuracy in other domains, such as traffic flow prediction and physiological signal reconstruction [41,42], but their application to structural monitoring data recovery remains relatively unexplored.

One-dimensional convolutional neural networks (1D-CNNs) and recurrent neural networks (RNNs) are among the most widely used deep learning frameworks for time-series modelling, including applications in structural health monitoring (SHM) [43]. 1D-CNNs are particularly effective in extracting local temporal features such as vibration modes and frequency-related signatures [44–46]. RNNs are capable of capturing long-range temporal dependencies in structural response signals [47]. Several studies have demonstrated the potential of 1D-CNNs for vibration-based damage detection and anomaly classification [45], whereas RNN-based approaches have been successfully applied to reconstruct missing measurements and predict dynamic responses [48,49]. More recently, hybrid CNN–RNN models have been introduced to leverage the complementary strengths of both architectures, achieving improved performance in domains where data are high-dimensional and strongly time-dependent, including SHM [50].

In recent years, several advanced deep learning architectures have been introduced across different engineering domains, demonstrating the rapid evolution and versatility of

AI-based diagnostic and reconstruction methods [51,52]. Attention-guided feature aggregation networks have been successfully applied to fault diagnosis of servo motor bearings, where attention mechanisms help emphasise discriminative temporal–frequency features and improve robustness under noisy operating conditions [53]. Data-driven machine learning frameworks have been employed for mechanical fault detection in robotic RV reducers using electrical current signature analysis, showing that AI models can effectively extract subtle degradation patterns from complex multichannel measurements [54,55]. These studies highlight a broader trend toward utilizing attention mechanisms, feature aggregation strategies, and domain-adapted learning frameworks to enhance the accuracy and reliability of condition monitoring. Building on these advancements, the present work contributes to the SHM field by leveraging a hybrid 1D-CNN–RNN architecture for reconstructing missing acceleration responses, extending the applicability of modern AI models to the challenge of incomplete structural vibration data.

In addition to fault detection and data recovery, AI has also become a cornerstone technology in the broader field of Prognostics and Health Management (PHM) [56]. Modern AI models enable not only the identification of abnormal behaviour but also the prediction of future degradation trends, remaining useful life (RUL), and system-level health evolution. Deep learning techniques have recently been applied to the prognostic health management of robotic strain wave gear reducers, where data-driven frameworks operating under variable-speed conditions can accurately model degradation trajectories and anticipate potential failures ahead of time. Such studies demonstrate that AI enhances PHM systems by providing scalable, self-learning, and real-time diagnostic and prognostic capabilities, especially in scenarios involving complex dynamics, non-stationary operating conditions, and high-dimensional sensor data [57]. Motivated by these advancements, the present study extends AI-driven methodologies to the SHM domain by focusing on the reconstruction of missing vibration data, an essential prerequisite for reliable monitoring, diagnosis, and prognostics in large-scale civil structures.

It is also important to note that the proposed data recovery approach operates within the cyber domain of a cyber–physical SHM system. While deep learning models have shown great potential for data reconstruction and signal restoration, there is a fundamental difference between recovering temporarily missing data from existing sensors and reproducing information from physically absent sensors. The latter is inherently limited because structural responses that were never measured cannot be fully inferred, particularly when the missing information is critical for identifying damage. Previous research has demonstrated that the number and spatial layout of sensors significantly impact the representativeness of CNN-based features and the sensitivity of SHM algorithms to structural changes [58]. Therefore, this study focuses on recovering incomplete or corrupted data from the available sensor network, assuming that sufficient spatial information remains within the system.

AI-based models have also been widely adopted in the structural assessment of advanced materials, particularly laminated composite structures used in aerospace, automotive, and mobility applications. Recent reviews have shown that intelligent computational methods, including deep learning and hybrid feature-learning frameworks, significantly enhance damage detection and condition evaluation in composite materials. These studies highlight that AI plays a central role across diverse SHM and PHM domains, further motivating the use of data-driven models for reliable health monitoring [59].

In this context, the proposed hybrid 1D-CNN–RNN framework supports the continuity and reliability of measurements in the cyber layer of a cyber–physical SHM architecture [60]. This perspective emphasises that the method complements, rather than replaces,

the physical sensing infrastructure, ensuring robust data streams for downstream tasks such as damage detection and modal analysis.

Only a few studies have directly addressed the problem of reconstructing missing or corrupted signals in structural health monitoring using deep learning techniques. Zhu et al. [48] developed a VMD- and SSA-enhanced Bi-LSTM approach that restores missing responses using spatial–temporal correlations among sensors and validated it on both real and public datasets. Continuous-missing scenarios on bridges have also been explored with GAN-based imputation frameworks, showing feasibility on real structures [61]. Jana et al. [62] proposed a CNN combined convolutional autoencoder framework for real-time sensor fault detection, localisation, and signal reconstruction, demonstrating accurate recovery on multichannel systems. Building upon these findings, the present study proposes a hybrid 1D-CNN–RNN model capable of learning both spatial correlations among sensor channels and temporal dependencies within vibration sequences. Unlike previous works, the proposed framework is validated on real-world field data from the Trai Hut Bridge in Vietnam, considers both single- and multi-channel loss scenarios, and systematically evaluates five network configurations to identify the most efficient architecture for accurate signal reconstruction. In this study, several distinctive features are introduced:

- A hybrid 1D CNN–RNN model is proposed for reconstructing missing SHM acceleration data, validated on real bridge monitoring data instead of simulated signals.
- Two practical sensor-loss scenarios—single-channel and multi-channel failures—are designed to reflect realistic field conditions.
- A systematic evaluation of model depth clarifies how network complexity influences accuracy and computational efficiency, offering guidance for selecting lightweight or deep configurations.
- The architecture is optimised for real-time and edge deployment, distinguishing it from prior CNN–LSTM/BiLSTM models developed mainly for offline analysis.

The remainder of this paper is organised as follows. Section 2 presents the methodology of the proposed hybrid 1D-CNN–RNN model, including data preprocessing, network architecture, and training strategy. Section 3 describes the case study using vibration data from the Trai Hut Bridge in Vietnam, along with the experimental setup under single- and multi-channel data loss scenarios. Finally, Section 4 concludes the paper by summarising the key findings and outlining directions for future research.

2. Methodology

2.1. One-Dimensional Convolutional Neural Network (1D-CNN)

A one-dimensional convolutional neural network (1D-CNN) is a specialised architecture designed to deal with sequential or time-series data. Unlike traditional 2D-CNNs used for image processing, the 1D-CNN applies convolutional operations along a single spatial or temporal dimension, making it highly suitable for analysing structural response signals collected from SHM systems.

In a 1D-CNN, the core operation is the convolution between an input sequence and a set of learnable filters (or kernels). Given an input time-series signal $X = [x_1, x_2, x_3, \ldots, x_n]$ and a filter $w = [w_1, w_2, w_3, \ldots, w_n]$ of size k, the convolution output at position i can be mathematically expressed as

$$s_i = (X \times w)_i = \sum_{j=1}^{k} w_j \times x_{i+j-1} \quad (1)$$

where x_i is the input value at position i; w_j is the weight of the filter at position j; s_i is the output (feature) at position i; k is the kernel size. The convolution operation allows

the network to automatically detect local patterns or features such as peaks, trends, or anomalies within the input signal.

2.2. Recurrent Neural Network (RNN)

A Recurrent Neural Network (RNN) is a class of artificial neural networks specifically designed to process sequential data, where the order and temporal dependencies among data points are essential. Unlike feedforward neural networks, RNN introduces a recurrent connection mechanism that allows information to be retained and propagated across time steps, making them highly suitable for modelling time-series data generated from SHM systems.

In a typical RNN architecture, at each temporal step t, the network receives an input vector x_t along with the preceding hidden state h_{t-1} to determine the updated hidden state h_t. This process can be mathematically formulated as

$$h_t = f(W_{xh}x_t + W_{hh}h_{t-1} + b_h) \tag{2}$$

$$y_t = g\Big(W_{hy}h_t + b_y\Big) \tag{3}$$

where x_t denotes the input at time step t; h_t represents the hidden state at time step t; y_t signifies the output at time step t; W_{xh}, W_{hh}, W_{hy} correspond to the weight matrices; b_h, b_y indicate the bias terms; $f(.)$ and $g(.)$ refer to the activation functions (typically *tanh* or *ReLU*).

2.3. Hybrid 1D-CNN–RNN

The hybrid 1D-CNN–RNN model was developed with the aim of simultaneously taking advantage of the ability to learn local features of the one-dimensional convolutional neural network (1D-CNN) and the ability to capture temporal dependencies of the recurrent neural network (RNN). The process of building the model consists of four main stages: data acquisition, data restructuring, dataset partitioning, and normalisation before training. Figure 1 shows the implementation process of the proposed method.

In the first stage, raw data are collected from the bridge vibration monitoring system, mainly in the form of multi-channel acceleration time series. Next, the data are converted into a proper format. This process includes segmenting the time series into windows of fixed length, with a defined stride to preserve continuity. Such restructuring helps to unify the input dimensions, while at the same time creating clear learning samples for the model. In each window, the masked data segments play the role of targets to be reconstructed during training.

After being formatted, the dataset is divided into three parts: training, validation, and testing. The partition ratio can be flexible but usually ensures that most of the data is used for training, while still keeping a sufficiently large portion for evaluation. This division helps to control overfitting and accurately reflect the model's generalization ability to unseen data.

Before being fed into the model, the data are normalised to eliminate differences in scale between sensor channels and to improve the stability of the optimisation process. Subsequently, the standardised data are processed through the 1D-CNN module to derive localised features. The features obtained from the 1D-CNN are then passed to the RNN block. Here, temporal dependencies are exploited. The RNN can remember information from previous steps, thereby enabling the model to reconstruct missing signal segments based on both local and global contexts.

Thanks to this combination, the 1D-CNN–RNN model not only restores missing data with high accuracy but also maintains the inherent dynamic structure of the vibration

signal. It is particularly important in the context of structural health monitoring, where the reliability and continuity of data are always of top priority.

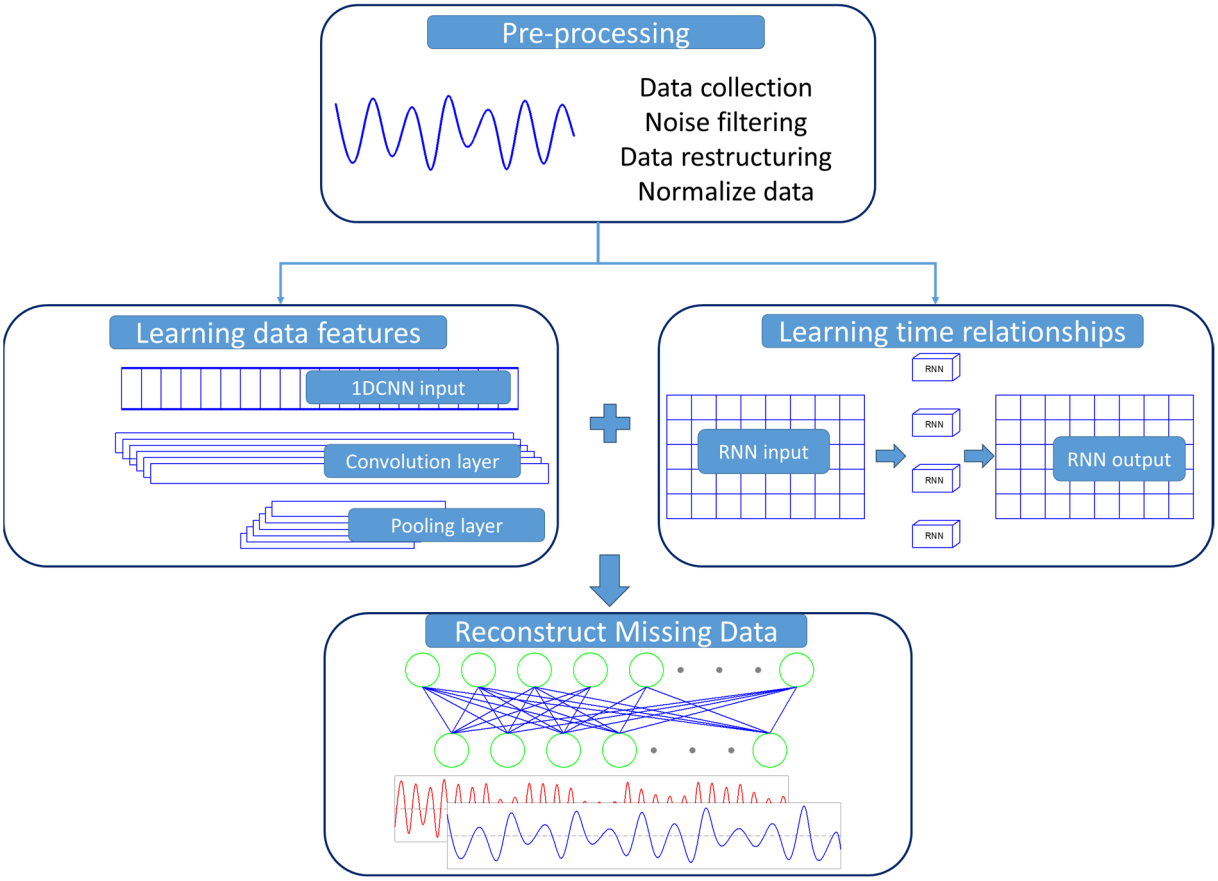


Figure 1. Algorithm implementation diagram.

2.4. Implementation Details

To enhance the reproducibility of the proposed hybrid 1D-CNN–RNN framework, this section provides detailed information about the data processing, network architecture, and training procedure. All experiments were implemented in Python 3.10 using TensorFlow 2.12 and Keras libraries. Model training and evaluation were conducted on a workstation equipped with an Intel Core i9 processor, 32 GB RAM, and an NVIDIA RTX 3080 GPU (10 GB VRAM) running the Windows 11 operating system.

The acceleration signals collected from the Trai Hut Bridge were segmented into overlapping time windows of 1024 samples with a stride of 512 samples, forming the training inputs. Each segment was normalised to zero mean and unit variance to eliminate scale differences between sensors and improve convergence stability. The dataset was randomly divided into 70% for training, 15% for validation, and 15% for testing.

To simulate missing data, specific sensor channels were intentionally masked. In the single-channel loss scenario, the entire signal of one channel was replaced with zeros while the others remained unchanged. In the multi-channel loss scenario, three channels were simultaneously replaced with zeros to represent concurrent sensor failures.

To optimise the reconstruction performance, the proposed hybrid 1D-CNN–RNN model was trained using the Mean Squared Error (MSE) as the objective function. MSE quantifies the average squared difference between the reconstructed and reference acceleration signals, thereby strongly penalising large deviations and promoting accurate recovery of both amplitude and temporal characteristics.

All models were trained using the Adam optimiser with an initial learning rate of 0.001, and the Mean Squared Error (MSE) as the objective (loss) function. The batch size was set to 50, and training was performed for up to 1000 epochs. Early stopping was employed with a patience of 50 epochs based on the validation loss to prevent overfitting and reduce computation time.

The model performance was quantitatively evaluated using the Mean Absolute Error (MAE) and the Coefficient of Determination (R^2) between the reconstructed and reference signals. Visual inspections of the reconstructed waveforms were also conducted to assess the model's capability in preserving both amplitude and phase characteristics. These combined metrics provide a comprehensive assessment of reconstruction accuracy across various network configurations and data loss scenarios.

3. Case Study

In this study, the Trai Hut bridge in Yen Bai province, Vietnam, will be used as a case study (Figure 2). The Trai Hut bridge is built in the area of An Binh and Dong An communes, Van Yen district, with the starting point connected to Provincial Road 163 (at Km55 + 150) and the ending point connected to Yen Bai—Khe Sang road (at Km56 + 750). The bridge has a total length of 277.4 m. It is situated on a grade IV mountainous road, as defined in the Vietnamese standard TCVN 4054:2005—Road Design Standards [63], which specifies a design speed of 30–40 km/h, with a roadbed width of 7.5 m.



(**a**) (**b**)

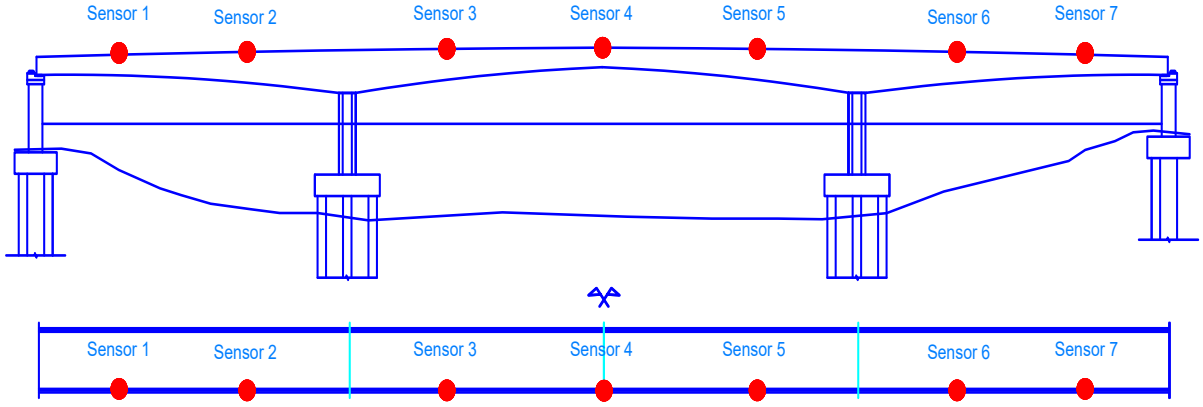
Figure 2. Trai Hut Bridge: (**a**) Surface of the bridge; (**b**) bridge's overview.

The bridge has a span configuration of 33 + 55 + 90 + 55 + 33 m, a total width of 9.0 m (including an 8.0 m carriageway and two 0.5 m sidewalks), and is designed for HL93 loading in accordance with the 22TCN-272-05 standard [64]. The superstructure consists of three continuous spans (55 + 90 + 55 m), where piers T2 and T3 are rigidly connected to prestressed reinforced concrete box girders with straight webs and variable depth ranging from 5.2 m above the piers to 2.2 m at midspan and girder ends. The bottom flange width is 5.0 m, and the top flange width is 8.7 m. The approach spans comprise two simple supported prestressed reinforced concrete I-girders, each 33 m in length, with four main girders spaced at 2.2 m and 1.65 m in height, topped with a 20 cm cast-in-place reinforced concrete deck slab with a 2% cross slope for drainage. The vertical alignment follows a curve of radius 2500 m and length 200.15 m, cresting at the midspan of the 90 m span, with a longitudinal gradient of 4% sloping towards both abutments. The deck is paved with a 7 cm asphalt concrete wearing course, with elastomeric bearings and expansion

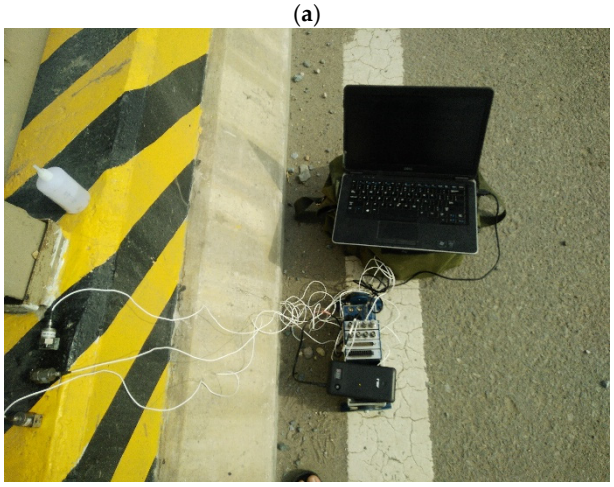
joints, complemented by steel guardrails, drainage, and lighting systems. The substructure comprises reinforced concrete wall-type abutments (M0 and M5) on 1.0 m diameter bored piles, solid reinforced concrete piers T1 and T4 on 1.0 m diameter bored piles equipped with movable bearings, and solid reinforced concrete piers T2 and T3 on 1.5 m diameter bored piles, rigidly connected to the continuous box girder system.

3.1. Bridge Vibration Measurement

An experimental vibration measurement campaign was conducted on the Trai Hut Bridge, with the sensor layout illustrated in Figure 3. A total of seven sensor positions were selected to record the structural vibrations of the bridge. The measurements were carried out under the influence of random loads, including traffic, wind, and other external forces. The sampling frequency was set at 1651 Hz. All signals from the sensors were transmitted to the data acquisition station via cable connections, where they were subsequently processed and displayed using specialised software on a dedicated computer.



(**a**)



(**b**)

Figure 3. Data gathering: (**a**) Measurement grid; (**b**) Sensor installation.

The sensors employed in this campaign were PCB 353B34 accelerometers. The installation locations were determined according to the predefined measurement scheme, after which signal cables were routed to the designated positions. The sensors were then mounted securely and connected to the data acquisition station. Prior to recording, the output signals were monitored, and data collection was initiated only once the parameters had stabilised. The data collection time during the campaign is about 30 min under normal bridge operating conditions. The station is located at sensor position 3. The sensors are connected to the measuring station via a signal cable system. The signal cable length is up

to 100 m, providing coverage of the entire bridge. Upon completion of the measurement campaign, a dataset comprising vibration responses at the selected locations on the bridge was obtained to serve the research objectives.

3.2. Single-Channel Sensor Data Reconstruction

To evaluate and verify the effectiveness of the proposed method, data loss scenarios with different levels will be built and tested. In the first research scenario, the phenomenon of single-channel data loss is simulated, where a sensor is damaged or stops working. Specifically, one data channel is intentionally corrupted by assigning all values to 0. The remaining data channels are kept as they were originally. In the single-channel loss scenario, the signal from sensor S4, located at the midspan of the main girder, was intentionally removed to simulate a complete data loss. This sensor was selected because its location corresponds to the point of maximum vertical acceleration under vehicular loading and exhibits a strong correlation with neighbouring sensors. Therefore, it provides a representative and challenging case for evaluating the model's ability to reconstruct critical structural responses.

The input data provided to the 1D-CNN–RNN hybrid model then includes only information from the non-corrupted channels. The desired output of the network is the data of the corrupted channel. This approach allows testing the model's ability to reconstruct and restore the missing signal from the information of the remaining channels. During training, the model is trained with 70% of the total collected data blocks. The remaining data is divided into 15% for testing and 15% for validation.

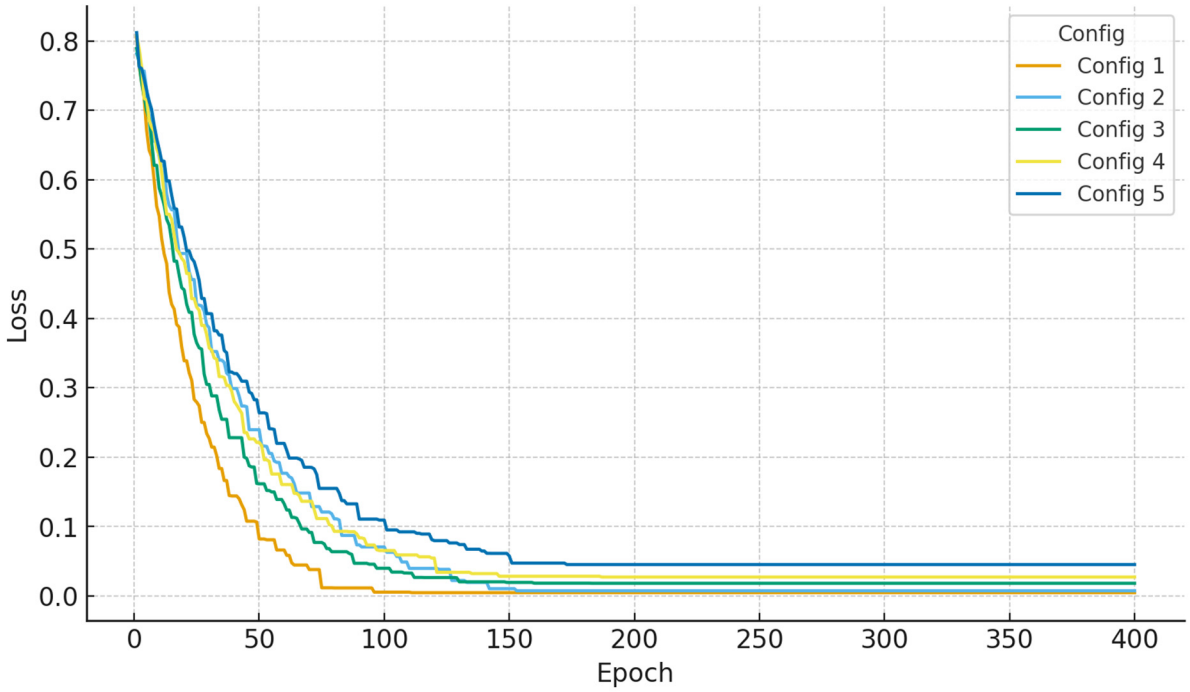
Network configurations of varying complexity were used to test the selection of the 1D-CNN–RNN architecture. A model that is too simplistic might not be able to extract complicated nonlinear data; therefore, selecting the right setup is crucial. Overfitting can easily occur when a model has too many parameters and is too complex. To assess the impact of model complexity on prediction accuracy, five network configurations were created using varying numbers of convolutional and fully connected layers (Table 1), along with adjustments to the number of filters, neurons, and dropout rate. The network hyperparameters, including the number of convolutional and recurrent layers, kernel sizes, hidden units, dropout rates, and learning rate, were tuned empirically through grid-based search using the training and validation subsets. The tuning was aimed at balancing accuracy and computational efficiency. Five configurations (Table 1) were defined to progressively increase model capacity from "small" (Config #1) to "very large" (Config #5). Validation loss (MAE) was used for model ranking. It was observed that larger networks (>1.5 M parameters) tended to overfit due to limited training samples (only 105 vibration segments), leading to degraded generalisation. It explains the observed "misbehaviour" of deeper configurations, which fit the noise rather than the structural correlation patterns.

Table 1. Details of tested network configurations.

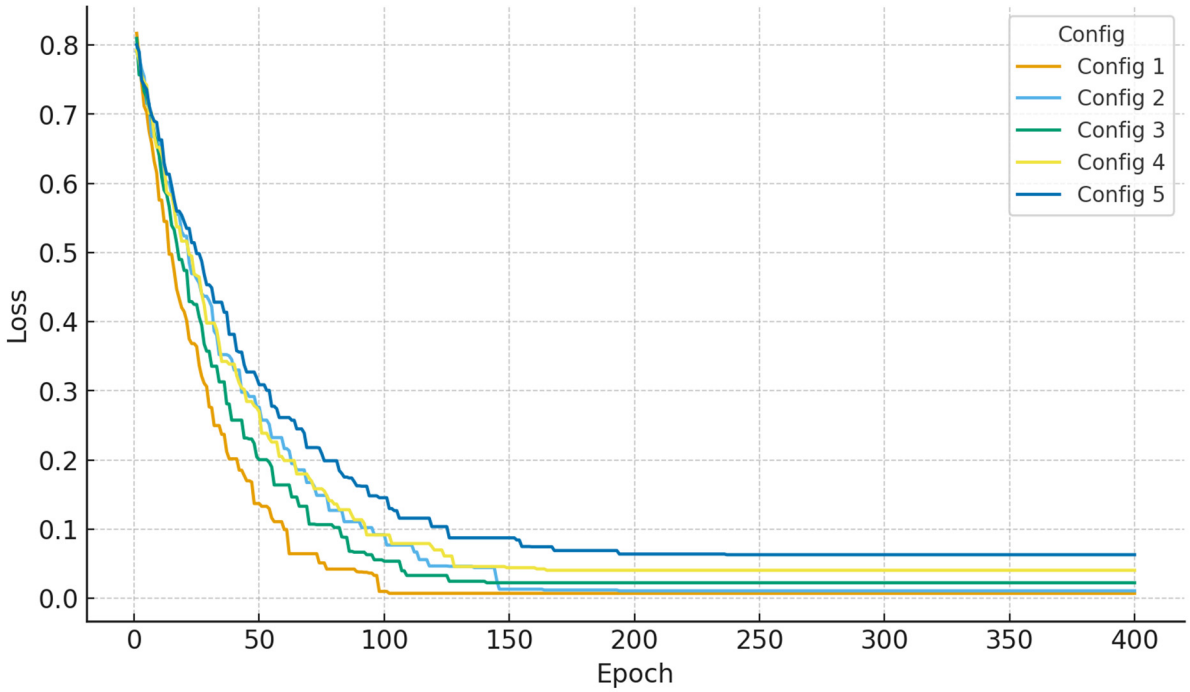
Configuration	CNN Layers	Filters Per CNN Layer	RNN Layers	Units Per RNN Layer	Dropout
Small (Config 1)	3	32–64–128	2	64–32	0.2
Medium-1 (Config 2)	3	64–128–256	3	128–128–64	0.2
Medium-2 (Config 3)	4	64–128–256–256	3	256–128–64	0.30
Large (Config 4)	4	64–128–256–512	3	256–128–64	0.3
Very-Large (Config 5)	5	64–128–256–512–512	4	512–256–128–64	0.35

The network configuration is used along with the ReLU activation function. The model is trained using the Adam optimisation algorithm with an initial learning rate of

0.001. The mean squared error (MSE) serves as the objective function. Training is conducted over 1000 iterations (epochs) with a batch size of 50. Following the training of various network configurations, Figure 4 displays the datasets' convergence curve in the single damage situation. For clarity, only the first 400 epochs are displayed, as the loss values remain nearly constant afterwards.

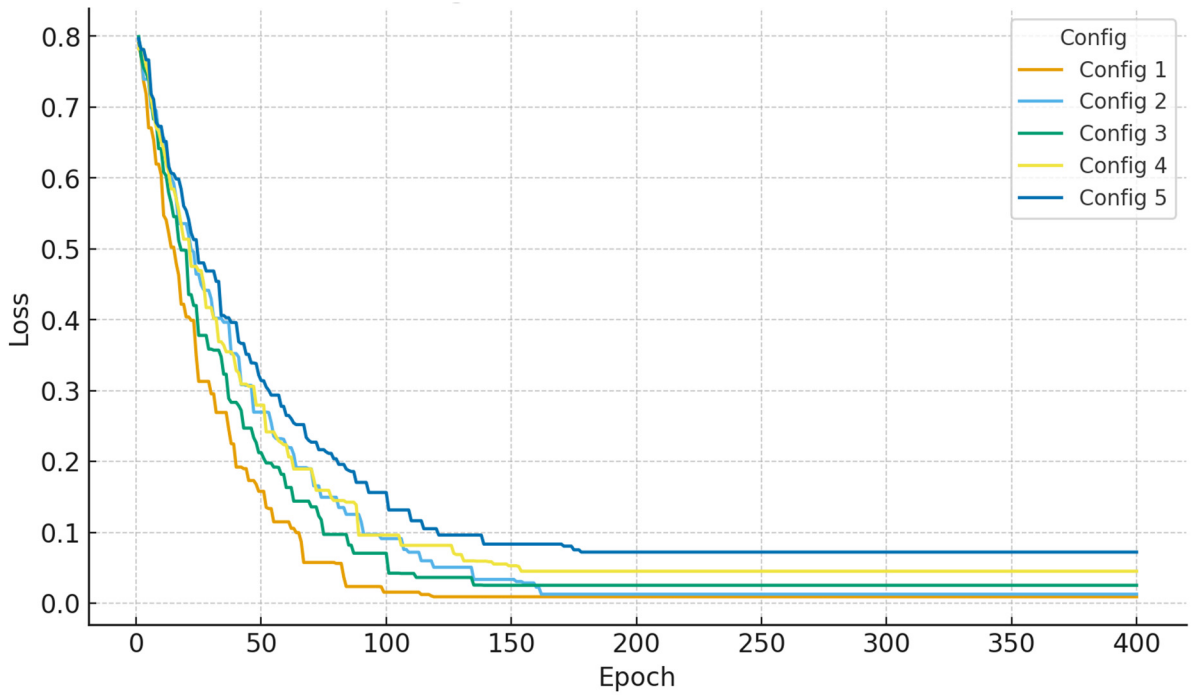


(**a**)



(**b**)

Figure 4. *Cont.*



(**c**)

Figure 4. Loss curve during training: (**a**) Training set; (**b**) Testing set; (**c**) Validating set (Single data loss).

In the initial epochs, loss rapidly decreases for all configurations. In particular, Configuration 1 begins to converge and gets closer to 0 after 93 epochs. After 158 epochs, Configuration 2 begins to converge and gets closer to 0. Following the initial phase, the training process's convergence is reflected in the loss levels, which progressively stabilise. The models that converge and get closest to 0 are those with configurations 1 and 2. The models that converge the most from 0 are those with configuration 5. Particularly on the test and validation sets, the Large and Very Large configurations exhibit higher loss values than configurations 1 and 2, and their gap is more than the training loss.

The Mean Absolute Error (MAE) values for the five assessed network configurations are displayed in Figure 5 for the training, testing, and validation sets. In all three datasets, the MAE gradually rises from Configuration 1 to Configuration 5. According to this pattern, the more intricate designs (Configurations 3–5) are more likely to overfit and have a harder time generalising to unknown data. With just slight variations across the training, testing, and validation sets, the MAE for Configurations 1 and 2 stays low. It indicates strong generalisation and consistent performance. Configurations 3, 4, and 5, on the other hand, exhibit noticeably greater MAE values, particularly on the validation set. Therefore, tiny profiles provide improved damage identification for single damage cases.

Figure 6 compares the reconstructed responses under the single-channel missing data scenario for different network configurations. Across all settings, the hybrid 1D-CNN–RNN model is able to reproduce the general waveform of the original signal, capturing both the amplitude and phase characteristics. However, clear differences appear among configurations: the smaller networks (Config. 1–2) provide reconstructions that are smoother and closer to the reference, whereas larger networks (Config. 4–5) show slight distortions and deviations, particularly at local peaks. It indicates that, when the loss of information is limited to one channel, excessive model complexity is not beneficial and may even introduce artifacts due to overfitting. In such cases, compact configurations are more effective, balancing accuracy and stability while requiring fewer computational resources.

Although the visual differences in Figures 5 and 6 may appear pronounced, particularly for Configurations 3 to 5, the quantitative reconstruction errors (MAE) remain within 4–7%. This apparent discrepancy primarily arises from the vertical scaling of the plots: small amplitude deviations are visually magnified when the signals are normalised and plotted within a limited range. The MAE values were computed based on normalised acceleration data over the entire time sequence, which averages out local deviations. Therefore, the numerical results and visual observations are consistent, confirming that the hybrid 1D-CNN–RNN framework maintains good reconstruction accuracy even for higher-capacity models.

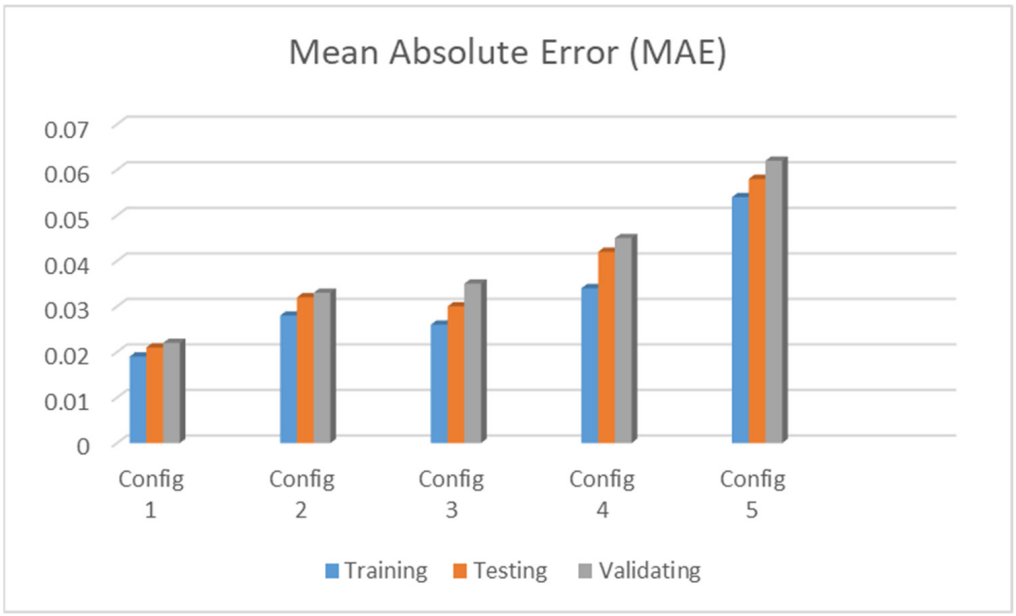


Figure 5. Mean Absolute Error (MAE) of configurations (Single data loss).

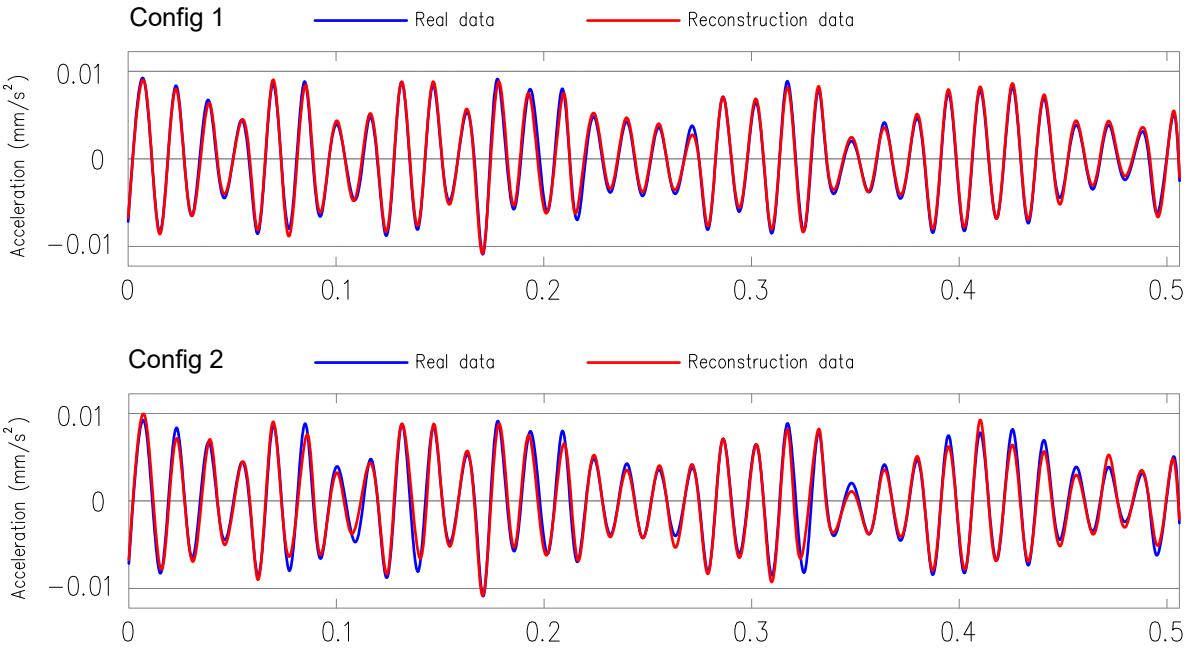


Figure 6. *Cont.*

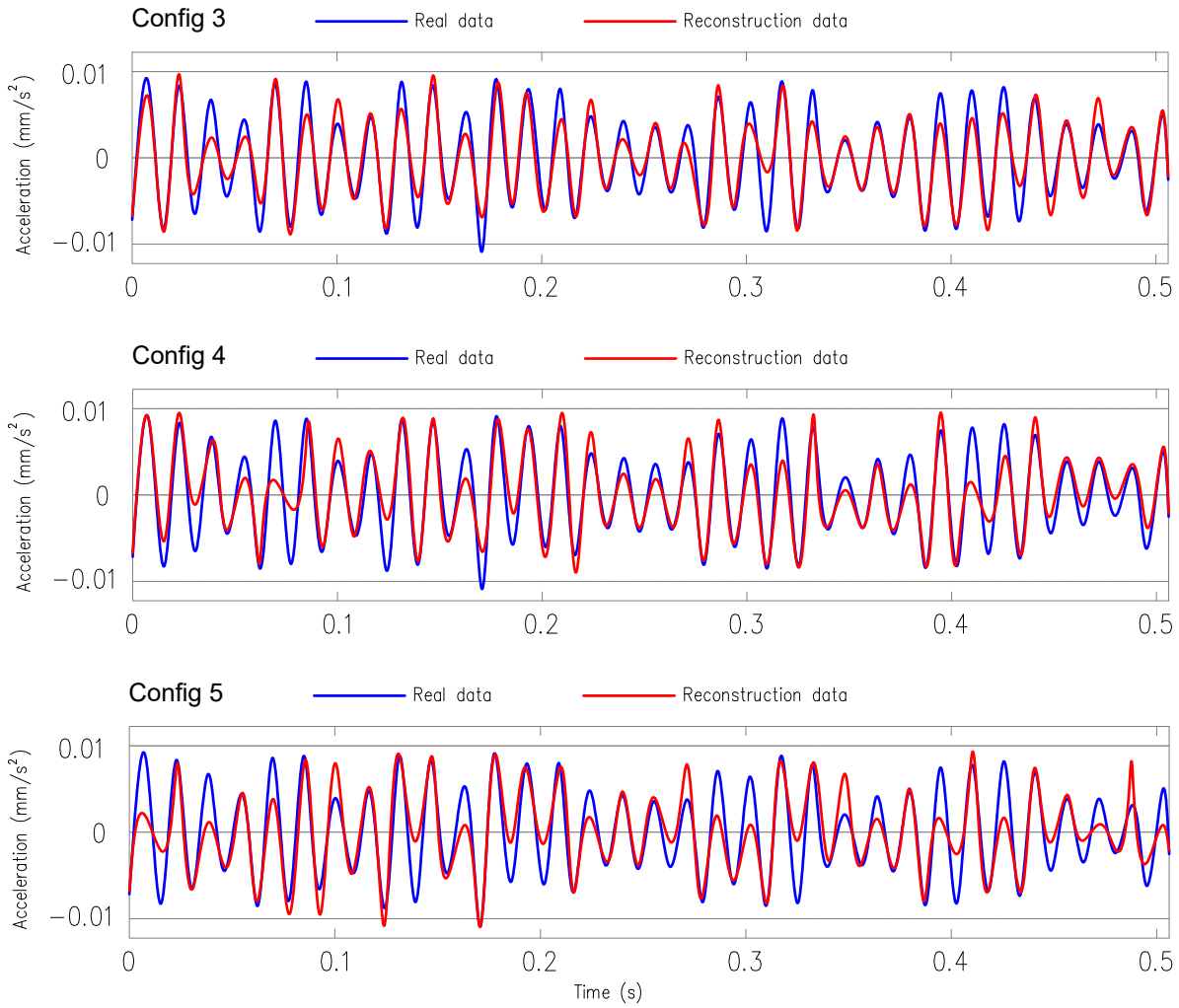


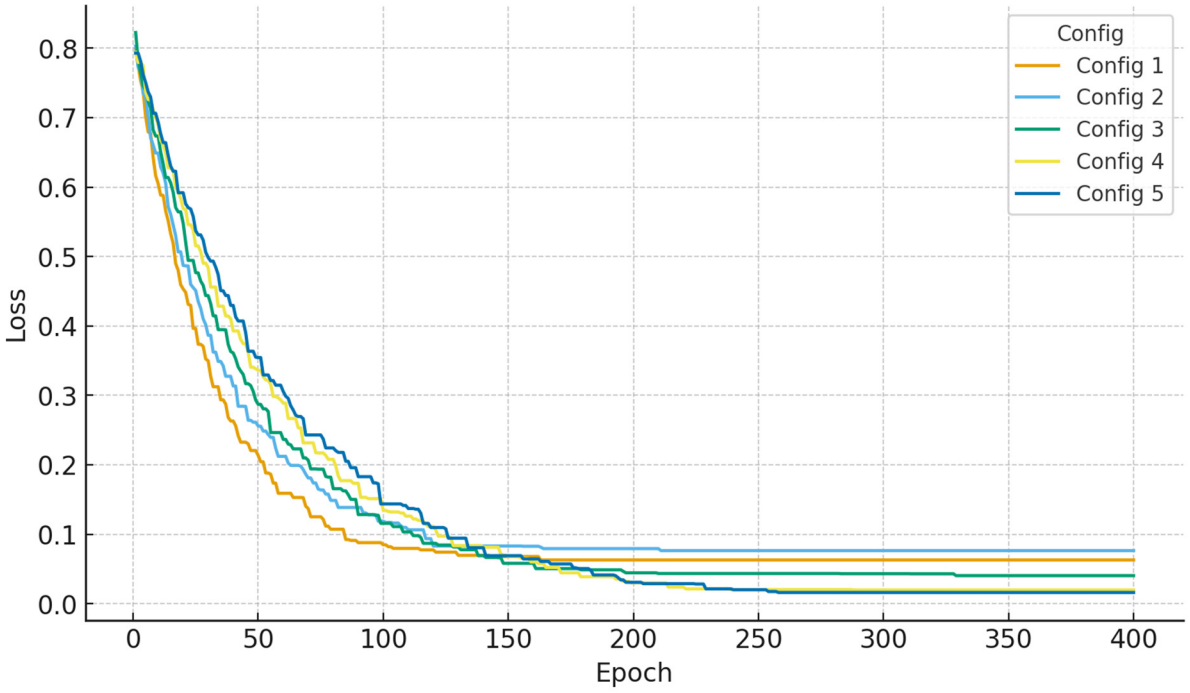
Figure 6. Data reconstructed from different configurations (Single data loss).

3.3. Multi-Channel Sensor Data Reconstruction

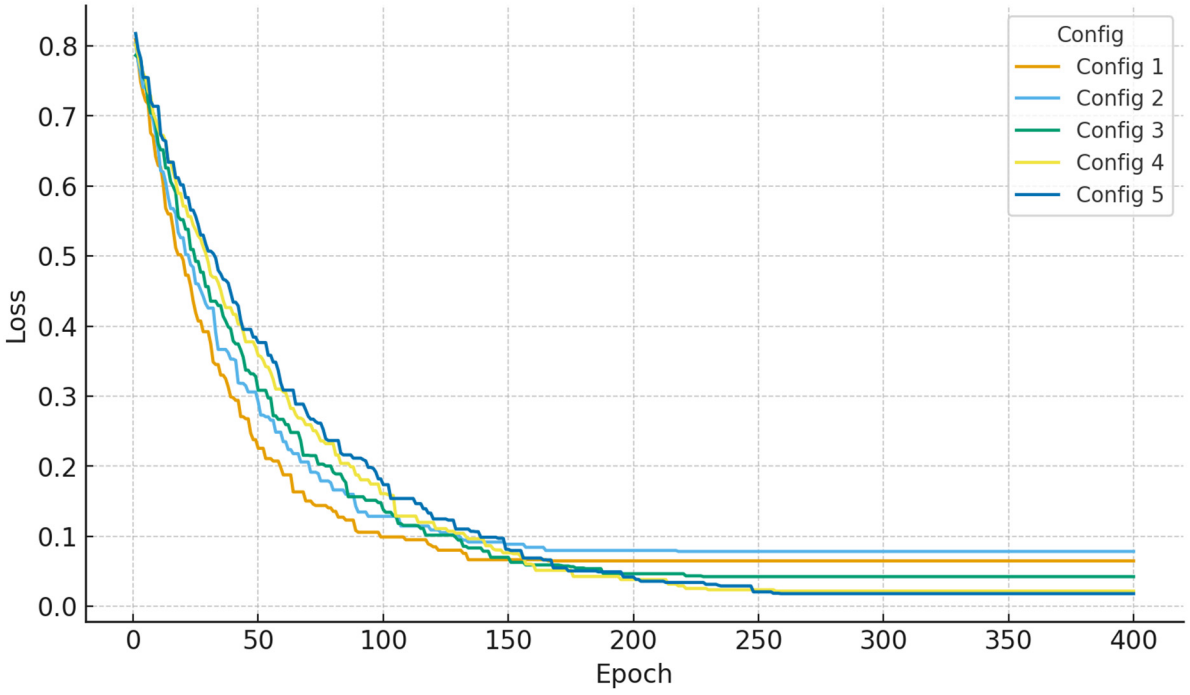
Following the assessment of the model in the context of single-sensor data loss, the investigation was subsequently broadened to consider the scenario involving the loss of multiple sensors. In this setting, the number of corrupted sensors was increased, leading to a reduction in the available input data and a corresponding increase in the amount of output data to be reconstructed. Specifically, a scenario involving the failure of three sensors was considered, in which their signals were set to zero, while the remaining sensors were preserved in their original state. In the multi-channel loss scenario, the signals from sensors S1, S2, and S4, positioned consecutively along the main span, were simultaneously removed. The network configurations were established in the same manner as in the single-sensor loss case. The training results for this scenario are presented in Figure 7. For clarity, only the first 400 epochs are displayed, as the loss values remain nearly constant afterwards for all configurations.

Figure 7 illustrates the convergence behaviour of the proposed networks under the multiple-channel data loss scenario. In all three subsets (training, testing, and validation), the loss decreases sharply during the initial epochs, indicating that the networks rapidly capture the underlying data patterns. After this steep decline, the curves gradually stabilise, reflecting convergence toward optimal solutions. When comparing different configurations, the larger networks (Configs 4 and 5) achieve lower final loss values than smaller configurations, demonstrating superior reconstruction capability under challenging data

loss conditions. Conversely, the smaller networks (Configs 1 and 2) converge more quickly but exhibit higher residual errors, suggesting limited representation capacity. Another observation is the consistency between the testing and validation curves, which closely follow the training trend without significant divergence. This behaviour indicates that the models maintain strong generalisation performance and are not severely overfitted, even in the multi-sensor loss scenario. The results confirm that increasing network depth and capacity enhances the robustness and accuracy of data recovery, particularly when multiple channels are corrupted.

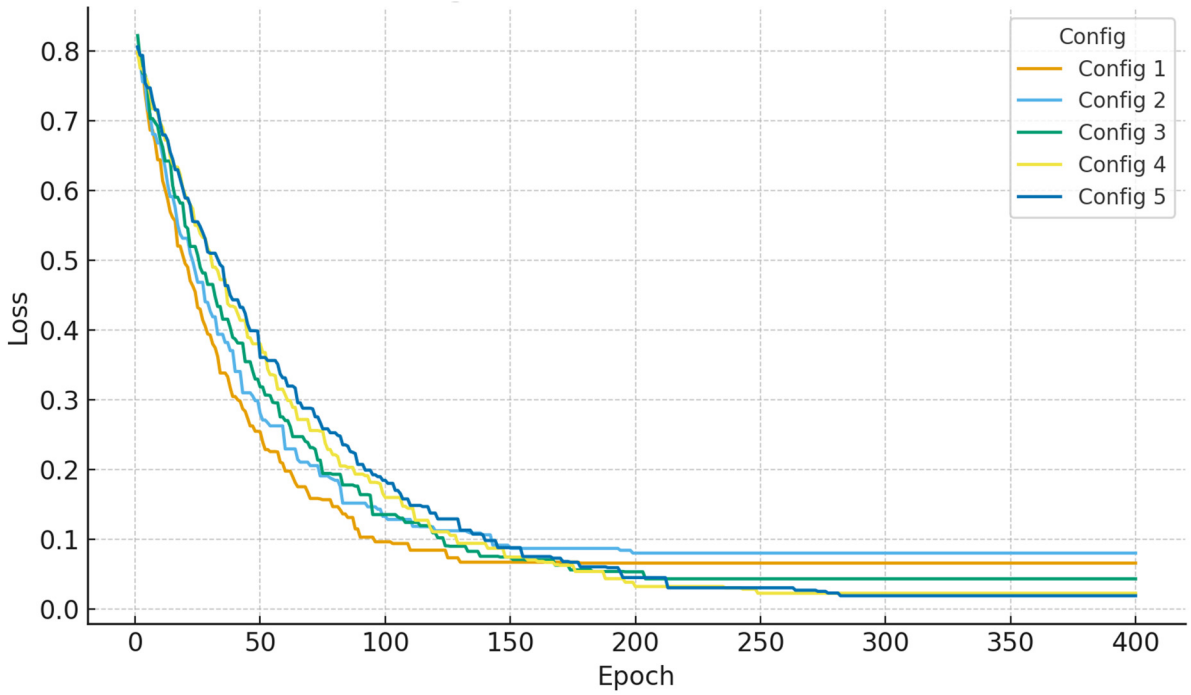


(**a**)



(**b**)

Figure 7. *Cont.*



(**c**)

Figure 7. Loss curve during training: (**a**) Training set; (**b**) Testing set; (**c**) Validating set (Multiple channel loss).

Although the training process was configured with a maximum of 1000 epochs, the convergence curves presented in Figures 4 and 7 show that the networks typically stabilised after approximately 350–400 epochs. This behaviour is a direct consequence of the characteristics of SHM vibration data. The temporal patterns are highly consistent, and the training set contains a limited number of vibration segments. The model requires a relatively long optimisation phase to refine the reconstruction of fine-scale dynamic features, particularly in deeper configurations. Nevertheless, the actual computational burden is effectively controlled using an early-stopping mechanism with a patience of 50 epochs. In practice, training automatically halts when the validation loss stops improving. This prevents unnecessary computation beyond the point of convergence. For most configurations, early stopping terminated the training process close to the 350–400 epoch range. It confirms that the model does not exhaust the full 1000-epoch limit. This validation mechanism ensures that computational resources are utilised efficiently while still allowing the network sufficient iterations to achieve stable and accurate reconstruction performance.

Figure 8 presents the MAE values of five different network configurations on the training, testing, and validation datasets. It can be observed that the smaller configurations (Config 1 and Config 2) yield relatively high errors, around 0.07 and 0.085, respectively. It reflects their limited capability in reconstructing signals when the number of layers and hidden units is restricted. In contrast, more complex configurations (Configs 3, 4, and 5) demonstrate superior performance, with MAE values reduced to below 0.05. Among them, Configs 4 and 5 achieve the lowest and nearly equivalent error levels, suggesting that once the depth of CNN–RNN layers and the number of parameters reach a certain threshold, model performance tends to stabilise without significant further improvement. It is also noteworthy that the differences among the three datasets (training, testing, and validation) are minimal across all configurations. It indicates that the networks stably learned the underlying features and maintained good generalisation ability, with no significant signs of overfitting.

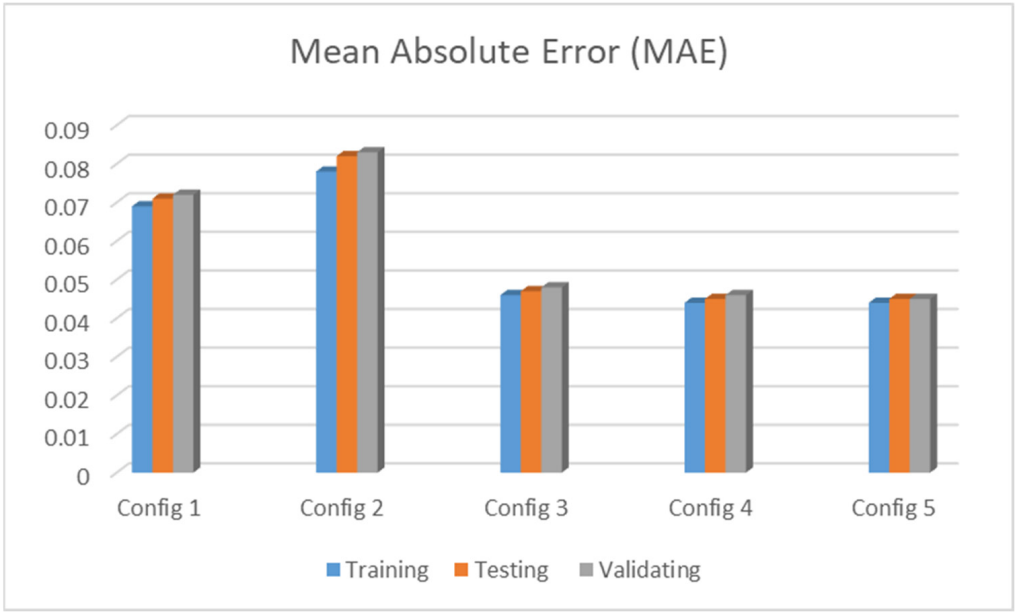


Figure 8. Mean Absolute Error (MAE) of configurations (Multiple channel loss).

Figure 9 illustrates the reconstructed acceleration responses when three sensor channels were simultaneously removed and recovered using Configuration 5. The reconstructed signals closely follow the original responses in both amplitude and phase, capturing the dominant dynamic patterns of the bridge. Although minor discrepancies remain in certain high-frequency components, the overall agreement confirms that the proposed hybrid 1D-CNN–RNN is able to exploit correlations across the remaining channels to restore physically meaningful responses even under severe multi-sensor loss. The results also demonstrate that a deeper configuration (Config. 5) provides sufficient representational capacity to model the complex dependencies required for multi-channel recovery, without producing unstable artifacts or unrealistic oscillations. This finding suggests that the proposed approach is reliable for practical SHM scenarios in which several sensors may fail simultaneously, thereby ensuring continuity of vibration monitoring and structural assessment.

The results from Figures 6 and 9 highlight the dependence of model performance on the extent of sensor loss. When only a single channel is missing, smaller configurations achieve reconstructions that are closer to the reference, showing that compact networks are sufficient and less prone to overfitting. In contrast, under multi-channel loss, a deeper configuration (Config. 5) is required to capture the complex inter-channel correlations and to restore realistic responses. This comparison emphasises that model selection should be adaptive to the severity of data loss: lightweight architectures are preferable for isolated sensor failures, while larger networks are justified when multiple sensors are simultaneously unavailable.

Compared with recent studies on signal reconstruction in SHM, the proposed hybrid 1D-CNN–RNN achieves comparable or superior accuracy with fewer parameters and faster convergence. These results demonstrate that the method is competitive with state-of-the-art deep learning approaches and suitable for practical SHM applications, where computational efficiency and model generalisation are crucial.

To further validate the effectiveness of the proposed hybrid 1D CNN–RNN architecture, several baseline models were implemented for comparison, including a pure CNN, a pure RNN (GRU-based), and traditional reconstruction algorithms such as linear interpolation and autoregressive (AR) models. These baselines were designed with comparable parameter sizes to ensure a fair evaluation.

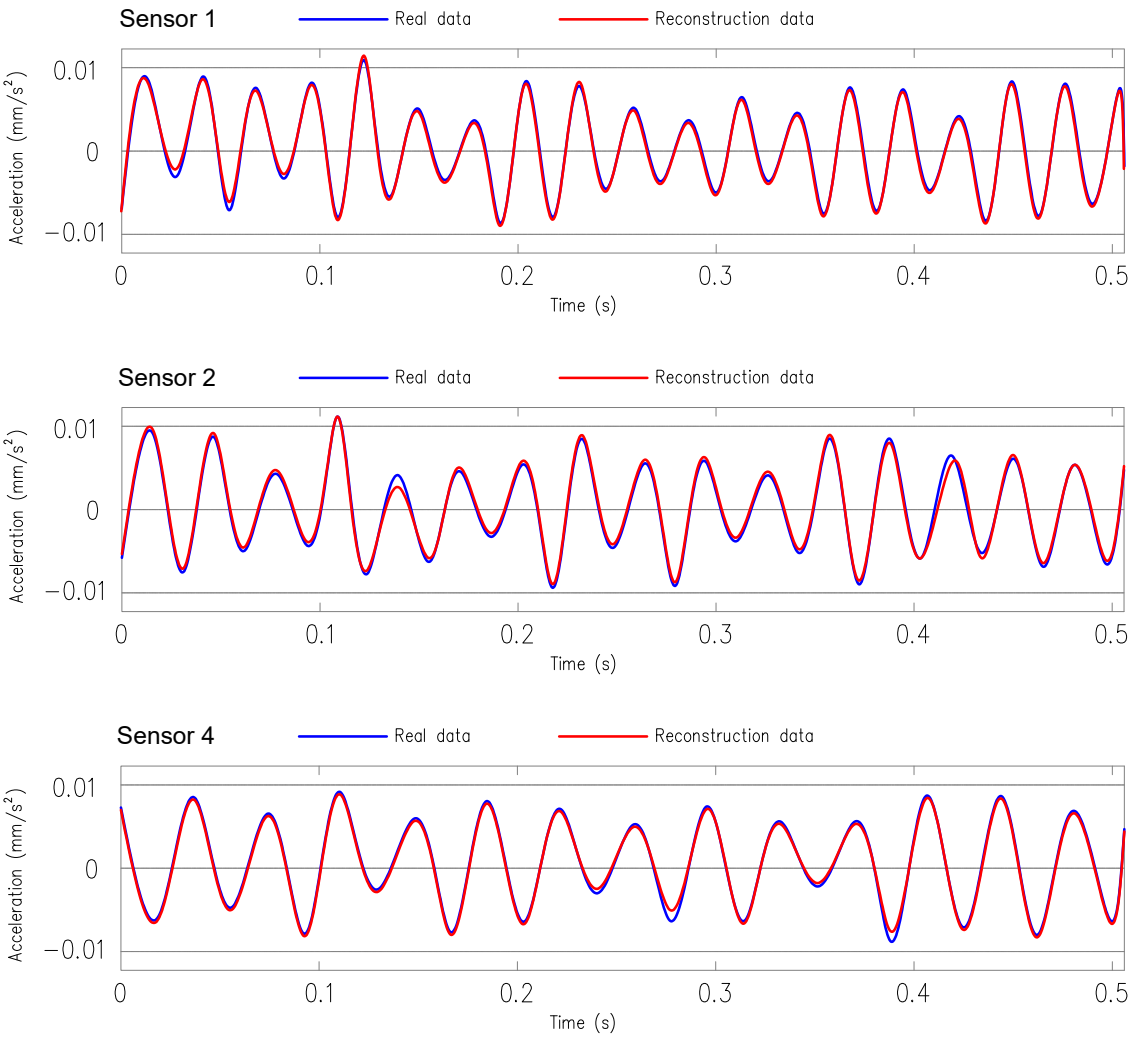


Figure 9. Data is reconstructed from configuration 5.

The proposed hybrid CNN–RNN consistently achieved the best reconstruction accuracy across both single-channel and multi-channel missing-data scenarios. Specifically, the hybrid model reduced the mean absolute error (MAE) by approximately 25–30% compared with the pure CNN and RNN models in the single-channel loss case, and by up to 40–50% under multi-channel loss conditions. Traditional interpolation and AR methods exhibited significantly larger errors, confirming their limited ability to capture nonlinear temporal and spatial dependencies among sensors.

These findings demonstrate that combining convolutional feature extraction with recurrent temporal modelling provides a clear advantage for structural health monitoring applications. The proposed CNN–RNN framework not only improves reconstruction accuracy but also maintains computational efficiency suitable for near–real-time field deployment.

Although the proposed hybrid 1D CNN–RNN model demonstrates strong performance in reconstructing missing SHM data, several limitations and practical considerations should be acknowledged:

- Dependence on training data: The model is trained using field data from a single bridge. While this ensures realistic noise and environmental conditions, it may limit generalisation to other structures or sensor layouts without additional transfer learning or re-training.

- Computational requirements: Although the proposed CNN–RNN remains relatively lightweight, training still requires GPU acceleration. On-site or edge deployment would benefit from model compression, pruning, or quantisation to reduce latency and memory usage.
- Potential overfitting risks: Despite early stopping and dropout layers, deeper configurations may still overfit limited SHM datasets. Expanding the dataset to multiple bridges or environmental conditions will be essential for robust generalisation.

4. Conclusions

This study proposed a hybrid 1D-CNN–RNN framework to reconstruct missing structural health monitoring (SHM) data, with application to acceleration responses measured on the Trai Hut Bridge. By simulating both single-channel and multi-channel data loss, the model performance was systematically examined under different network configurations. The results showed that compact configurations were sufficient to recover accurate responses when only one sensor was missing, while deeper networks provided superior reconstructions in the more challenging case of multi-sensor loss. In both scenarios, the reconstructed signals closely followed the original measurements in amplitude and phase, indicating that the proposed method can maintain the fundamental dynamic behaviour of the structure. The key contributions of this research can be summarised as follows:

(1) Developed a 1D-CNN–RNN model that combines local feature extraction with temporal dependency learning for reconstructing missing SHM data.
(2) Investigated the effects of single-channel versus multi-channel data loss using multiple network configurations, providing insights into the relationship between model size and recovery performance.
(3) Applied and validated the proposed framework on real acceleration measurements from the real bridge case study, demonstrating practical feasibility for large-scale SHM systems.
(4) A real-world case study was conducted using vibration data from the Trai Hut Bridge in Vietnam. Five network configurations with varying depths were examined under single- and multi-channel loss scenarios. The results confirm that the proposed method can accurately reconstruct lost signals. For single-channel loss, the best configuration achieved an MAE = 0.019 m/s^2 and R^2 = 0.987, while for multi-channel loss, a deeper network yielded an MAE = 0.044 m/s^2 and R^2 = 0.974.
(5) Highlighted that compact models are more effective for isolated sensor failures, while deeper networks are advantageous when multiple sensors fail simultaneously.

Future research may extend the framework to other bridge types and operating conditions, integrate physics-informed constraints, and develop adaptive strategies that automatically adjust network capacity according to the severity of sensor loss.

Author Contributions: Conceptualisation, N.T.T.N., J.C.M. and S.D.N.; methodology, N.T.T.N. and S.D.N.; software, N.T.T.N.; validation, N.T.T.N., J.C.M. and S.D.N.; formal analysis, J.C.M. and S.D.N.; investigation, N.T.T.N. and S.D.N.; resources, N.T.T.N. and S.D.N.; data curation, N.T.T.N. and S.D.N.; writing—original draft preparation, N.T.T.N., J.C.M. and S.D.N.; writing—review and editing, N.T.T.N., J.C.M. and S.D.N.; visualisation, N.T.T.N. and S.D.N.; supervision, J.C.M. and S.D.N.; project administration, N.T.T.N., J.C.M. and S.D.N.; funding acquisition, J.C.M. and S.D.N. All authors have read and agreed to the published version of the manuscript.

Funding: This research received no external funding.

Data Availability Statement: The data presented in this study are available at the request of the corresponding author due to the host institution's rules.

Acknowledgments: The authors would like to thank the University of Transport Technology, Hanoi, Vietnam.

Conflicts of Interest: The authors declare no conflicts of interest.

References

1. Zhang, B.; Ren, Y.; He, S.; Gao, Z.; Li, B.; Song, J. A Review of Methods and Applications in Structural Health Monitoring (SHM) for Bridges. *Measurement* **2025**, *245*, 116575. [CrossRef]
2. Ye, X.W.; Su, Y.H.; Han, J.P. Structural Health Monitoring of Civil Infrastructure Using Optical Fiber Sensing Technology: A Comprehensive Review. *Sci. World J.* **2014**, *2014*, 652329. [CrossRef]
3. Ribeiro, D.; Rakoczy, A.M.; Cabral, R.; Hoskere, V.; Narazaki, Y.; Santos, R.; Tondo, G.; Gonzalez, L.; Matos, J.C.; Massao Futai, M.; et al. Methodologies for Remote Bridge Inspection—Review. *Sensors* **2025**, *25*, 5708. [CrossRef]
4. Tran, M.Q.; Sousa, H.S.; Nguyen, N.T.C.; Nguyen, Q.H.; Campos e Matos, J. Opportunities and Challenges of Digital Twins in Structural Health Monitoring. In *Proceedings of the 4th International Conference on Sustainability in Civil Engineering*; ICSCE 2022. Lecture Notes in Civil Engineering; Nguyen-Xuan, T., Nguyen-Viet, T., Bui-Tien, T., Nguyen-Quang, T., Roeck, G., Eds.; Springer: Singapore, 2024; Volume 344. [CrossRef]
5. Bento, A.M.; Minh, T.Q.; Ferradosa, T.; Sousa, H.S.; Nguyen, H.X.; Campos e Matos, J. Study on the Model to Determine Riverbed Scour and the Influence of Bridge Construction on Riverbed Deformation. In *Analytical and Experimental Methods in Mechanical and Civil Engineering*; OES 2023. Structural Integrity; Pavlou, D., Ed.; Springer: Cham, Switzerland, 2024; Volume 28. [CrossRef]
6. Tran, M.Q.; Sousa, H.S.; Matos, J.; Fernandes, S.; Nguyen, Q.T.; Dang, S.N. Finite Element Model Updating for Composite Plate Structures Using Particle Swarm Optimization Algorithm. *Appl. Sci.* **2023**, *13*, 7719. [CrossRef]
7. Nguyen, N.T.C.; Le, A.T.; Bui, H.N.; Van Ngo, T.; Bui, H.P.; Tran, M.Q. Determine Train Load and Speed Based on Dynamic Displacement Results. *J. Mater. Eng. Struct. «JMES»* **2025**, *11*, 543–552.
8. Quang, M.T.; Cam, N.N.T.; Duc, B.N.; Bui, H.N.; Van, T.N. Monitoring and Evaluation of Tension Loss in Cables of Cable-Stayed Bridges: A Case Study. In Proceedings of the IABSE Congress: Beyond Structural Engineering in a Changing World, San Jose, Costa Rica, 25–27 September 2024. [CrossRef]
9. Tran, M.Q.; Sousa, H.S.; Ngo, T.V.; Nguyen, B.D.; Nguyen, Q.T.; Nguyen, H.X.; Baron, E.; Matos, J.; Dang, S.N. Structural Assessment Based on Vibration Measurement Test Combined with an Artificial Neural Network for the Steel Truss Bridge. *Appl. Sci.* **2023**, *13*, 7484. [CrossRef]
10. Sohn, H.; Farrar, C.; Hemez, F.M.; Czarnecki, J.J. A Review of Structural Health Monitoring Literature 1996–2001. *Los Alamos Natl. Lab.* **2003**, *1*, 10–1298.
11. Farrar, C.R.; Worden, K. *Structural Health Monitoring: A Machine Learning Perspective*; John Wiley Sons Ltd.: New York, NY, USA, 2012. [CrossRef]
12. Ho, V.L.; Khatir, S.; Roeck, G.D.; Bui-Tien, T.; Wahab, M.A. Finite Element Model Updating of a Cable-Stayed Bridge Using Metaheuristic Algorithms Combined with Morris Method for Sensitivity Analysis. *Smart Struct. Syst.* **2020**, *26*, 451–468. [CrossRef]
13. Ho, V.L.; Hoang, T.N.; De Roeck, G.; Bui, T.T.; Abdel Wahab, M. Effects of Measuring Techniques on the Accuracy of Estimating Cable Tension in a Cable-Stay Bridge. In *Proceedings of the 13th International Conference on Damage Assessment of Structures*; Lecture Notes in Mechanical Engineering; Wahab, M., Ed.; Springer: Singapore, 2020. [CrossRef]
14. Zhang, L.; Liu, J.; Sun, X.; Jiang, X.; Zou, Z.; Li, X. A Review of Bridge Structural Health Monitoring Based on Different Optical Acquisition Modules. *Measurement* **2025**, *257*, 118922. [CrossRef]
15. Nguyen, N.T.; Tran, M.Q.; Sousa, H.S.; Van Ngo, T.; Matos, J.C. Damage Detection of Structural Based on Indirect Vibration Measurement Results Combined with Artificial Neural Network. *J. Mater. Eng. Struct. «JMES»* **2022**, *9*, 403–410.
16. Biju, V.G.; Schmitt, A.-M.; Engelmann, B. Assessing the Influence of Sensor-Induced Noise on Machine-Learning-Based Changeover Detection in CNC Machines. *Sensors* **2024**, *24*, 330. [CrossRef]
17. Mardanshahi, A.; Sreekumar, A.; Yang, X.; Barman, S.K.; Chronopoulos, D. Sensing Techniques for Structural Health Monitoring: A State-of-the-Art Review on Performance Criteria and New-Generation Technologies. *Sensors* **2025**, *25*, 1424. [CrossRef]
18. Sun, Z.; Mahmoodian, M.; Sidiq, A.; Jayasinghe, S.; Shahrivar, F.; Setunge, S. Optimal Sensor Placement for Structural Health Monitoring: A Comprehensive Review. *J. Sens. Actuator Netw.* **2025**, *14*, 22. [CrossRef]
19. Chen, S.-Y.; Wang, Y.-W.; Ni, Y.-Q. Gross Outlier Removal and Fault Data Recovery for SHM Data of Dynamic Responses by an Annihilating Filter-Based Hankel-Structured Robust PCA Method. *Struct. Control Health Monit.* **2022**, *29*, e3144. [CrossRef]
20. García-Laencina, P.J.; Sancho-Gómez, J.L.; Figueiras-Vidal, A.R. Pattern Classification with Missing Data: A Review. *Neural Comput. Applic.* **2010**, *19*, 263–282. [CrossRef]
21. Peeters, B.; De Roeck, G. Stochastic System Identification for Operational Modal Analysis: A Review. *J. Dyn. Syst. Meas. Control* **2001**, *123*, 659–667. [CrossRef]

22. Gao, K.; Weng, S.; Zhu, H.-P. Recovery of Missing Strain Data under Multiple Time-Varying Effects Using IMM Kalman Filtering. *Eng. Struct.* **2025**, *329*, 119830. [CrossRef]
23. Chen, S.-Y.; Wang, Y.-W.; Ni, Y.-Q. Multi-Channel Lost Data Recovery for Structural Health Monitoring by Structured Low-Rank Matrix Completion. *Struct. Health Monit.* **2025**, 14759217251319514. [CrossRef]
24. Royston, P.; White, I.R. Multiple Imputation by Chained Equations (MICE): Implementation in Stata. *J. Stat. Softw.* **2011**, *45*, 1–20. [CrossRef]
25. Ding, Y.; Ye, X.-W.; Guo, Y.; Zhang, R.; Ma, Z. Probabilistic Method for Wind Speed Prediction and Statistics Distribution Inference Based on SHM Data-Driven. *Probabilistic Eng. Mech.* **2023**, *73*, 103475. [CrossRef]
26. Ding, Y.; He, Z.-X.; Zhou, S.-X. Multi-Dimensional Models for Predicting the Chloride Diffusion in Concrete Exposed to Marine Tidal Zone: Methodology, Numerical Simulation and Application. *Comput. Concr.* **2024**, *34*, 169–178. [CrossRef]
27. Paschalis, P.; Giokaris, N.D.; Karabarbounis, A.; Loudos, G.K.; Maintas, D.; Papanicolas, C.N.; Spanoudaki, V.; Tsoumpas, C.; Stiliaris, E. Tomographic Image Reconstruction Using Artificial Neural Networks. *Nucl. Instrum. Methods Phys. Res. Sect. Accel. Spectrometers Detect. Assoc. Equip.* **2004**, *527*, 211–215. [CrossRef]
28. Tran, M.Q.; Sousa, H.S.; Matos, J.C. Application of AI Tools in Creating Datasets from a Real Data Component for Structural Health Monitoring. In *Data Driven Methods for Civil Structural Health Monitoring and Resilience*; CRC Press: Boca Raton, FL, USA, 2023; pp. 223–241. [CrossRef]
29. Fanous, M.J.; Casteleiro Costa, P.; Işıl, Ç.; Huang, L.; Ozcan, A. Neural Network-Based Processing and Reconstruction of Compromised Biophotonic Image Data. *Light Sci. Appl.* **2024**, *13*, 231. [CrossRef] [PubMed]
30. Minh, T.Q.; Van, T.N.; Nguyen, H.X.; Nguyễn, Q. Enhancing the Structural Health Monitoring (SHM) through Data Reconstruction: Integrating 1D Convolutional Neural Networks (1DCNN) with Bidirectional Long Short-Term Memory Networks (Bi-LSTM). *Eng. Struct.* **2025**, *340*, 120767. [CrossRef]
31. Minh, T.Q.; Matos, J.C.; Sousa, H.S.; Ngoc, S.D.; Van, T.N.; Nguyen, H.X.; Nguyễn, Q. Data Reconstruction Leverages One-Dimensional Convolutional Neural Networks (1DCNN) Combined with Long Short-Term Memory (LSTM) Networks for Structural Health Monitoring (SHM). *Measurement* **2025**, *253*, 117810. [CrossRef]
32. Chen, C.; Tang, L.; Lu, Y.; Wang, Y.; Liu, Z.; Liu, Y.; Zhou, L.; Jiang, Z.; Yang, B. Reconstruction of Long-Term Strain Data for Structural Health Monitoring with a Hybrid Deep-Learning and Autoregressive Model Considering Thermal Effects. *Eng. Struct.* **2023**, *285*, 116063. [CrossRef]
33. Oh, B.; Park, H.; Glisic, B. Prediction of Long-Term Strain in Concrete Structure Using Convolutional Neural Networks, Air Temperature and Time Stamp of Measurements. *Autom. Constr.* **2021**, *126*, 103665. [CrossRef]
34. Lei, X.; Sun, L.; Xia, Y. Lost Data Reconstruction for Structural Health Monitoring Using Deep Convolutional Generative Adversarial Networks. *Struct. Health Monit.* **2020**, *20*, 2069–2087. [CrossRef]
35. Nhung, N.T.C.; Bui, H.N.; Quang, M.T. A Novel Hybrid Deep Learning-Based Approach for Sensor Data Recovery in Structural Health Monitoring. *Int. J. Integr. Eng.* **2025**, *17*, 190–203. [CrossRef]
36. Nhung, N.T.C.; Bui, H.N.; Minh, T.Q. Enhancing Recovery of Structural Health Monitoring Data Using CNN Combined with GRU. *Infrastructures* **2024**, *9*, 205. [CrossRef]
37. Nhung, N.T.C.; Nguyen, H.B.; Minh, T.Q. Reconstructing Health Monitoring Data of Railway Truss Bridges Using One-Dimensional Convolutional Neural Networks. *Eng. Technol. Appl. Sci. Res.* **2024**, *14*, 15510–15514. [CrossRef]
38. Lu, Y.; Tang, L.; Chen, C.; Zhou, L.; Liu, Z.; Liu, Y.; Jiang, Z.; Yang, B. Reconstruction of Long-Term Acceleration Response for Long-Span Bridges Based on BiLSTM Networks. *Eng. Struct.* **2023**, *285*, 116000. [CrossRef]
39. Fan, G.; Li, J.; Hao, H. Lost Data Recovery for Structural Health Monitoring Based on Convolutional Neural Networks. *Struct. Control Health Monit.* **2019**, *26*, e2433. [CrossRef]
40. Oh, B.; Glisic, B.; Kim, Y.; Park, H. Convolutional Neural Network-Based Data Recovery Method for Structural Health Monitoring. *Struct. Health Monit.* **2020**, *19*, 1821–1838. [CrossRef]
41. Zhang, J.; Yang, Y.; Wu, X.; Li, S. Spatio-Temporal Graph Convolutional Networks for Traffic Flow Forecasting. *Sci. Rep.* **2025**, *15*, 24299. [CrossRef]
42. Che, Z.; Purushotham, S.; Cho, K.; Sontag, D.; Liu, Y. Recurrent Neural Networks for Multivariate Time Series with Missing Values. *Sci. Rep.* **2018**, *8*, 6085. [CrossRef]
43. Naghashi, V.; Boukadoum, M.; Diallo, A.B. Should We Reconsider RNNs for Time-Series Forecasting? *AI* **2025**, *6*, 90. [CrossRef]
44. Kiranyaz, S.; Ince, T.; Gabbouj, M. Real-Time Patient-Specific ECG Classification by 1-D Convolutional Neural Networks. *IEEE Trans. Biomed. Eng.* **2016**, *63*, 664–675. [CrossRef]
45. Abdeljaber, O.; Kiranyaz, S.; Gabbouj, M.; Inman, D.J. Real-Time Vibration-Based Structural Damage Detection Using 1D Convolutional Neural Networks. *J. Sound Vib.* **2017**, *388*, 154–170. [CrossRef]
46. Tran, V.L.; Vo, T.C.; Nguyen, T.Q. One-Dimensional Convolutional Neural Network for Damage Detection of Structures Using Time Series Data. *Asian J. Civ. Eng.* **2024**, *25*, 827–860. [CrossRef]

47. Cho, K.; van Merrienboer, B.; Gulcehre, C.; Bahdanau, D.; Bougares, F.; Schwenk, H.; Bengio, Y. Learning Phrase Representations Using RNN Encoder-Decoder for Statistical Machine Translation. *arXiv* **2014**. [CrossRef]
48. Zhu, S.; Miao, J.; Chen, W.; Liu, C.; Weng, C.; Luo, Y. Reconstructing Missing Data Using a Bi-LSTM Model Based on VMD and SSA for Structural Health Monitoring. *Buildings* **2024**, *14*, 251. [CrossRef]
49. Hewamalage, H.; Bergmeir, C.; Bandara, K. Recurrent Neural Networks for Time Series Forecasting: Current Status and Future Directions. *Int. J. Forecast.* **2021**, *37*, 388–427. [CrossRef]
50. Cha, Y.-J.; Lewis, J.; Büyük, O. Deep Learning-Based Structural Health Monitoring. *Autom. Constr.* **2024**, *161*, 105328. [CrossRef]
51. Lv, H.; Chen, J.; Pan, T.; Zhang, T.; Feng, Y.; Liu, S. Attention Mechanism in Intelligent Fault Diagnosis of Machinery: A Review of Technique and Application. *Measurement* **2022**, *199*, 111594. [CrossRef]
52. Wu, H.; Triebe, M.J.; Sutherland, J.W. A Transformer-Based Approach for Novel Fault Detection and Fault Classification/Diagnosis in Manufacturing: A Rotary System Application. *J. Manuf. Syst.* **2023**, *67*, 439–452. [CrossRef]
53. Raouf, I.; Kumar, P.; Kim, H.S. Deep Learning-Based Fault Diagnosis of Servo Motor Bearing Using the Attention-Guided Feature Aggregation Network. *Expert Syst. Appl.* **2024**, *258*, 125137. [CrossRef]
54. Feng, Z.; E, Y.; Chen, X.; Zhang, Y. Motor Current Analytical Models and Signature Analysis for Rotate Vector Reducer Fault Diagnosis. *Mech. Syst. Signal Process.* **2025**, *239*, 113240. [CrossRef]
55. Rohan, A.; Raouf, I.; Kim, H.S. Rotate Vector (RV) Reducer Fault Detection and Diagnosis System: Towards Component Level Prognostics and Health Management (PHM). *Sensors* **2020**, *20*, 6845. [CrossRef]
56. Raouf, I.; Lee, H.; Noh, Y.R.; Youn, B.D.; Kim, H.S. Prognostic Health Management of the Robotic Strain Wave Gear Reducer Based on Variable Speed of Operation: A Data-Driven via Deep Learning Approach. *J. Comput. Des. Eng.* **2022**, *9*, 1775–1788. [CrossRef]
57. Lee, H.; Raouf, I.; Song, J.; Kim, H.S.; Lee, S. Prognostics and Health Management of the Robotic Servo-Motor under Variable Operating Conditions. *Mathematics* **2023**, *11*, 398. [CrossRef]
58. Almutairi, M.; Nikitas, N.; Abdeljaber, O.; Avci, O.; Bocian, M. A Methodological Approach towards Evaluating Structural Damage Severity Using 1D CNNs. *Structures* **2021**, *34*, 4435–4446. [CrossRef]
59. Azad, M.M.; Cheon, Y.; Raouf, I.; Khalid, S. Intelligent Computational Methods for Damage Detection of Laminated Composite Structures for Mobility Applications: A Comprehensive Review. *Arch. Comput. Methods Eng.* **2024**, *32*, 441–469. [CrossRef]
60. Doghri, W.; Saddoud, A.; Chaari Fourati, L. Cyber-Physical Systems for Structural Health Monitoring: Sensing Technologies and Intelligent Computing. *J. Supercomput.* **2022**, *78*, 766–809. [CrossRef]
61. Jiang, H.; Wan, C.; Yang, K.; Ding, Y.; Xue, S. Continuous Missing Data Imputation with Incomplete Dataset by Generative Adversarial Networks–Based Unsupervised Learning for Long-Term Bridge Health Monitoring. *Struct. Health Monit.* **2021**, *21*, 1093–1109. [CrossRef]
62. Jana, D.; Patil, J.; Herkal, S.; Nagarajaiah, S.; Duenas-Osorio, L. CNN and Convolutional Autoencoder (CAE) Based Real-Time Sensor Fault Detection, Localization, and Correction. *Mech. Syst. Signal Process.* **2022**, *169*, 108723. [CrossRef]
63. *TCVN 4054:2005*; Vietnam Road Design Standards. Vietnam Standard: Hanoi, Vietnam, 2005.
64. *22TCN272:2005*; Bridge Design Standards. Ministry of Transport: Hanoi, Vietnam, 2005.

Disclaimer/Publisher's Note: The statements, opinions and data contained in all publications are solely those of the individual author(s) and contributor(s) and not of MDPI and/or the editor(s). MDPI and/or the editor(s) disclaim responsibility for any injury to people or property resulting from any ideas, methods, instructions or products referred to in the content.